Applied Catalysis B: Environmental 115–116 (2012) 7–15

Contents lists available at SciVerse ScienceDirect

Applied Catalysis B: Environmental

journal homepage: www.elsevier.com/locate/apcatb

Supported Pd catalysts for solvent-free benzyl alcohol selective oxidation: Effects of calcination pretreatments and reconstruction of Pd sites

Xueming Wang, Guangjun Wu, Naijia Guan, Landong Li*

Key Laboratory of Advanced Energy Materials Chemistry (Ministry of Education), College of Chemistry, Nankai University, Tianjin 300071, PR China

ARTICLE INFO

Article history:
Received 24 October 2011
Received in revised form
18 November 2011
Accepted 7 December 2011
Available online 16 December 2011

Keywords:
Supported Pd catalysts
Selective oxidation
Calcination pretreatments
Reconstruction

ABSTRACT

Pd catalysts supported on Al_2O_3 and TiO_2 have been prepared by wet impregnation and studied for the solvent-free selective oxidation of benzyl alcohol by molecular oxygen. High activity as well as high selectivity to benzaldehyde can be obtained and the calcination pretreatments show distinct effects on the catalytic activities of supported Pd catalysts. Supported Pd catalysts before and after benzyl alcohol oxidation are characterized by means of XPS, FTIR spectra of CO adsorption and O_2-TPD. The results clearly show that the palladium sites in supported Pd catalysts undergo reconstruction during benzyl alcohol oxidation. Based on the catalytic and characterization results, the possible benzyl alcohol oxidation reaction pathways and the active palladium sites in supported Pd catalysts for benzyl alcohol oxidation are discussed.

1. Introduction

The selective oxidation of alcohols to carbonyl compounds is one of the most important organic transformations, which is of great interest not only to fundamental organic synthesis but also to fine chemical industry [1]. Conventionally, stoichiometric oxidants, e.g. dichromate and permanganate, are employed in the process of alcohols oxidation. These oxidants are usually toxic and/or expensive, and large amounts of wastes are produced together with the desired products. With the economic and environmental concerns, it is proposed to use molecular oxygen as clean and cheap oxidant to realize so-called green oxidation process [2,3]. Homogeneous catalysts based on metal complexes can offer high activity and selectivity in the selective oxidation of alcohols using molecular oxygen as oxidant [4,5]. Compared to homogeneous catalytic process, heterogeneous catalytic process shows great advantages in catalyst separation and recycling, and therefore is more feasible for industrial application. In recent years, numerous catalyst systems, e.g. Mn catalysts [6], Co catalysts [7], Ru catalysts [8–11], Au catalysts [12–17] and Pd catalysts [18–29], have been developed for the heterogeneous selective oxidation of alcohols with molecular oxygen as oxidant. Among all the catalysts reported, Pd catalysts appear to be very promising ones because high activity and high selectivity can be obtained simultaneously.

Despite extensive researches on Pd catalysts for alcohol selective oxidation, the discrimination of active palladium sites is still controversial. In early studies, a general proposal is that metallic palladium species are the active sites and the dehydrogenation step is prevalent during alcohol oxidation on Pd catalysts [3,26]. While for hydroxyapatite-supported palladium clusters, Kaneda et al. proposed that the oxidation of alcohols occurred primarily at coordinately unsaturated palladium atoms on the surface of the nanoclusters at the reaction temperature of 363 K [19]. Based on the results from in situ X-ray absorption fine-structure spectroscopy, Lee et al. proposed that surface palladium oxide layer was essential for the high activity and reduced palladium sites performed poorly in the oxidative dehydrogenation of alcohol at 333 K [27,28]. In great contrast, Grunwaldt et al. reported that palladium oxides exhibited hardly any catalytic activity for alcohol oxidation at 323 K, whereas metallic palladium particles were much more active based on the results from in situ X-ray absorption spectroscopy [29]. In our opinion, the controversies on the active palladium sites are very much dependent on the reaction conditions employed for alcohol oxidation. Typically, the reaction temperatures and the solvents employed may influence the process of alcohol oxidation distinctly and therefore lead to dissimilar deduction of active palladium sites. Besides, the structure and physical–chemical properties of Pd catalysts may also influence the oxidation of alcohols.

For an ideal green oxidation process, the oxidation reaction should be performed under mild conditions using molecular oxygen as oxidant and be free of any solvent or additives. In the present study, we will report the transformation of benzyl alcohol to benzaldehyde over Pd/Al_2O_3 and Pd/TiO_2 via ideal green

* Corresponding author. Tel.: +86 22 2350 0341; fax: +86 22 2350 0341.
E-mail address: lild@nankai.edu.cn (L. Li).

0926-3373/$ – see front matter © 2011 Elsevier B.V. All rights reserved.
doi:10.1016/j.apcatb.2011.12.011

oxidation process. Here, Al_2O_3 and TiO_2 are selected as representative supports since they are the most common supports for Pd catalysts. Al_2O_3 is typical non-reducible support, while TiO_2 is typical reducible support. The effects of calcination pretreatments on the catalytic activity are investigated and the reconstruction of palladium sites during benzyl alcohol oxidation process is observed. Based on the characterization and catalytic results, the benzyl alcohol oxidation pathways and the active palladium sites are discussed.

2. Experimental

2.1. Preparation of supported Pd catalysts

Commercial TiO_2 (Degussa P25, 70% anatase, 30% rutile, surface area: 49 m^2/g) and γ-Al_2O_3 (Sinopec, surface area: 167 m^2/g) were used as catalyst supports. Palladium species were introduced to the support by wet impregnation with $PdCl_2$ as precursor. In a typical preparation process of Pd/Al_2O_3, 30 mL $PdCl_2$ aqueous solution (Pd concentration: 1.0 mg/mL) was added to 1 g γ-Al_2O_3 support and then evaporated in a rotary evaporator at constant temperature of 353 K. The as-obtained samples were carefully washed with deionized water, dried at 353 K overnight and then subjected to different calcination pretreatments.

The calcination processes were performed at 673 K for 4 h under different atmospheres, i.e. oxidizing atmosphere 10% O_2/He, reducing atmosphere 10% H_2/He and inert atmosphere 10% N_2/He. The final product was labeled based on the calcination atmosphere. For example, Pd/Al_2O_3–O represented Pd/Al_2O_3 sample calcined in 10% O_2/He, Pd/TiO_2–N represented Pd/TiO_2 sample calcined in 10% N_2/He and Pd/TiO_2–H represented Pd/TiO_2 sample calcined in 10% H_2/He.

2.2. Characterization of supported Pd catalysts

The exact palladium loadings in supported Pd catalysts were analyzed on an IRIS Advantage inductively coupled plasma atomic emission spectrometer (ICP-AES).

X-ray diffraction (XRD) patterns of the samples were recorded on a Bruker D8 diffractometer with Cu$K\alpha$ radiation (λ = 1.5418 Å) from 5° to 80° with a scan speed of $2\theta = 6.0°$/min.

Nitrogen adsorption/desorption measurements of samples were performed at 77 K on a NOVA 1000 e (Quantachrome Instruments) after outgassing at 473 K under vacuum for 12 h. The specific surface area was calculated with the Brunauer–Emmett–Teller (BET) equation.

Transmission electron microscopy (TEM) images of samples were acquired on a JEOL 2010 transmission electron microscope at an acceleration voltage of 200 kV. A few drops of alcohol suspension containing the catalyst samples were placed on a carbon-coated copper grid, followed by evaporation at ambient temperature.

The temperature-programmed desorption of oxygen (O_2-TPD) on supported Pd catalysts were performed on the chemisorption analyzer. The samples were pre-treated in 10% O_2/He at 473 K for 2 h and then cooled down to room temperature in the same flow. After He purge for 30 min at 323 K, the temperature-programmed desorption experiments were conducted in He flow from 323 to 873 K at a heating rate of 10 K/min.

X-ray photoelectron spectra (XPS) of samples were recorded on a Kratos Axis Ultra DLD spectrometer with a monochromated Al Kα X-ray source ($h\nu$ = 1486.6 eV), hybrid (magnetic/electrostatic) optics and a multi-channel plate and delay line detector (DLD). All spectra were recorded using an aperture slot of 300 μm × 700 μm, survey spectra were recorded with a pass energy of 160 eV and high-resolution spectra with a pass energy of 40 eV. Accurate binding energies (±0.1 eV) were determined with respect to the position of the adventitious C 1s peak at 284.8 eV.

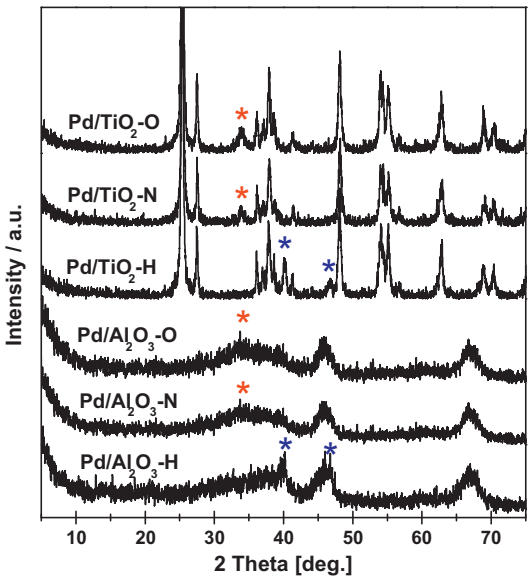

Fig. 1. XRD patterns of supported Pd catalysts after different calcination pretreatments.

FTIR spectra of CO adsorption on samples were collected on the Bruker Tensor 27 spectrometer with 128 scans at a resolution of 4 cm^{-1}. A self-supporting pellet made of the catalyst sample was placed in the IR flow cell and the background spectrum was taken at room temperature. After the He stream was switched to a gas mixture containing 1% CO in He at a total flow rate of 30 mL/min, a series of time-dependent FTIR spectra of CO adsorption on the samples were sequentially recorded.

2.3. Selective oxidation of benzyl alcohol

The solvent-free selective oxidation of benzyl alcohol over supported Pd catalysts was performed under atmosphere pressure. In each experiment, catalyst sample of 100 mg was dispersed in 0.3 mol benzyl alcohol in a three-necked batch reactor with a reflux condenser under stirring. The suspension was kept at 393 K with oxygen bubbled in at a flow-rate 50 mL/min. After the reaction, the catalyst sample was removed from the reaction mixture by centrifugation and the products were analyzed by gas chromatography (Shimadzu GC-2010 Plus with DB-624 capillary column) as well as GC-MS (Shimadzu GCMS-QP2010 SE). The carbon balance in liquid phase is found to be >95% for all tests, and therefore the formation of volatile products, e.g. CO and CO_2, is neglected.

3. Results and discussion

3.1. Characterization of supported Pd catalysts

The XRD patterns of Pd/Al_2O_3 and Pd/TiO_2 after different calcination pretreatments are shown in Fig. 1. Typical diffraction peaks corresponding to γ-Al_2O_3 support (JCPDS 29-1486) are observed in all Pd/Al_2O_3 samples. Besides, diffraction peak at 33.8° corresponding to palladium oxide (JCPDS 41-1107) can be observed in Pd/Al_2O_3 calcined in O_2/He and N_2/He, indicating the formation of palladium oxide. While for Pd/Al_2O_3 calcined in H_2/He, diffraction peaks at 40.1° and 46.5° corresponding to metallic Pd (JCPDS 46-1043) are observed in addition to the diffraction peaks corresponding to γ-Al_2O_3 support. Quite similar results can be obtained

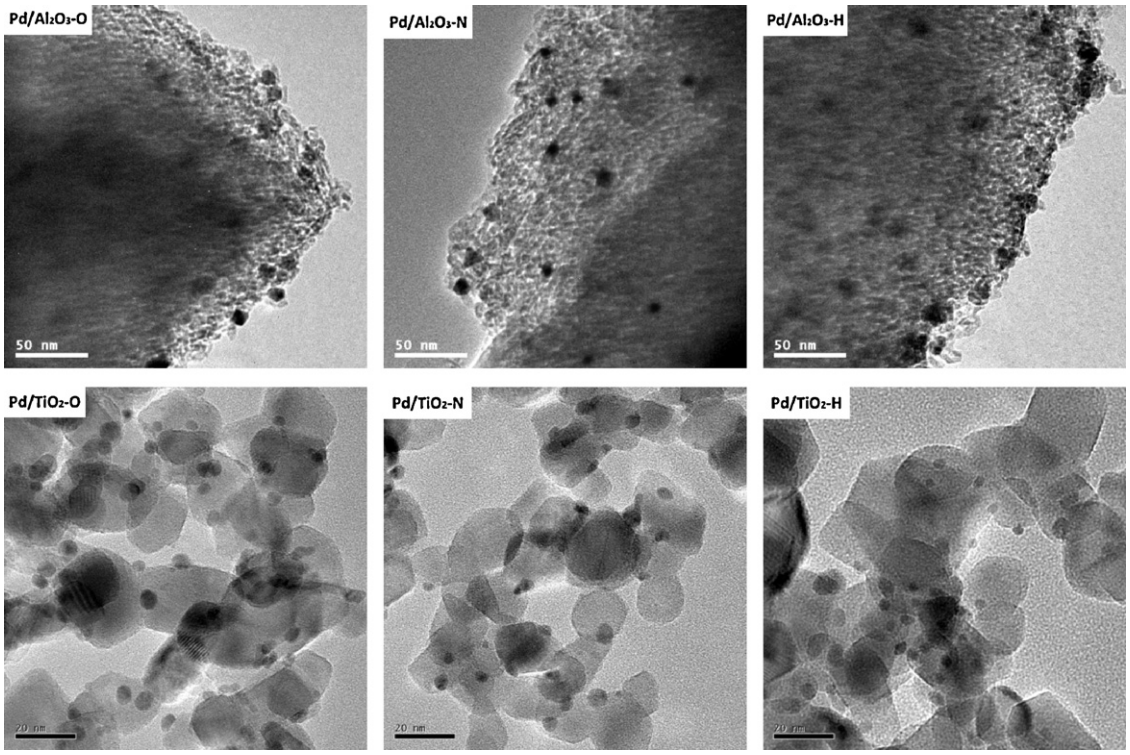

Fig. 2. TEM images of Pd/Al_2O_3 and Pd/TiO_2 after different calcination pretreatments.

on Pd/TiO_2 samples after different calcination pretreatments. That is, palladium oxide is formed during calcination in O_2/He and N_2/He, while metallic palladium is formed during calcination in H_2/He.

The TEM images of Pd/Al_2O_3 and Pd/TiO_2 after different calcination pretreatments are shown in Fig. 2. It is seen that palladium tends to form nano-sized clusters on Al_2O_3 and TiO_2 support. For Pd/Al_2O_3 calcined under different atmospheres, palladium clusters with averages diameters of 6–8 nm are observed to disperse on the support. While for Pd/TiO_2 calcined under different atmospheres, slightly smaller and more uniform palladium clusters of 4–5 nm are observed to disperse on the surface of TiO_2. After reaction of benzyl alcohol oxidation, the sizes of supported Pd clusters are kept nearly unchanged, as shown in Fig. S1. The physical–chemical properties of Pd/Al_2O_3 and Pd/TiO_2 samples after different calcination pretreatments are summarized in Table 1.

3.2. Catalytic activities in benzyl alcohol selective oxidation

Fig. 3 shows the time-dependent of benzyl alcohol conversions catalyzed by Pd/Al_2O_3 and Pd/TiO_2. It is seen that benzyl alcohol conversions increase distinctly with prolonged reaction time for all catalysts. The major product is benzaldehyde (>90%), while small quantity of benzoic acid and benzylbenzoate (<10%) can be detected as by-products. The by-product benzoic acid comes from the over-oxidation of aiming product benzaldehyde by molecular oxygen, while the by-product of benzylbenzoate comes from the esterification between benzyl alcohol and benzoic acid. The leaching of Pd in liquid phase is found to be <1 ppm in all catalytic tests, and therefore the activity contribution from leached Pd complex can be neglected. For Pd/Al_2O_3, the calcination atmospheres show distinct impacts on the catalytic activity. The highest benzyl alcohol conversion is achieved on Pd/Al_2O_3–N, followed by Pd/Al_2O_3–O and then Pd/Al_2O_3–H. For Pd/TiO_2, similar benzyl alcohol conversions are achieved on Pd/TiO_2–O and Pd/TiO_2–N. Interestingly, almost no benzyl alcohol conversion can be observed on Pd/TiO_2–H, probably due to the formation of the strong metal–support interaction and the encapsulation of palladium on TiO_2 during calcination in H_2/He [30,31].

Based on the catalytic results presented in Fig. 3, we conclude that selective oxidation of benzyl alcohol to benzaldehyde can be realized on Pd/Al_2O_3 and Pd/TiO_2 catalysts with high activity and

Table 1
Physical–chemical properties of supported Pd catalysts after different pretreatments.

Samples	Pd loading (%)[a]	Pd cluster size (nm)[b]	Surface area (m^2/g)	Pd existence states[c]
Pd/Al_2O_3–O	2.51	6.6	151	PdO
Pd/Al_2O_3–N	2.56	6.5	144	PdO
Pd/Al_2O–H	2.68	7.2	148	Pd^0
Pd/TiO_2–O	2.59	4.4	44	PdO_x
Pd/TiO_2–N	2.57	4.5	42	PdO_x
Pd/TiO_2–H	2.75	4.8	39	Pd^0 and PdO_x

[a] Determined by ICP.
[b] Average size observed by TEM.
[c] Determined by XPS.

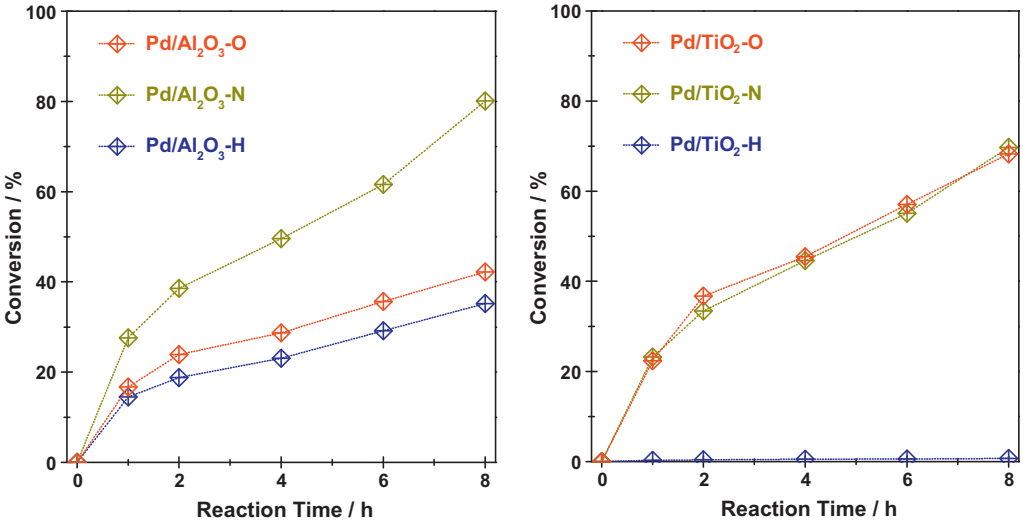

Fig. 3. Selective oxidation of benzyl alcohol over Pd/Al_2O_3 and Pd/TiO_2 at 393 K.

selectivity via ideal green oxidation process, i.e. under solvent-free conditions and with molecular oxygen as oxidant. The calcination pretreatments of samples show distinct impacts on the catalytic activity for benzyl alcohol selective oxidation.

3.3. Reconstruction of Pd sites during benzyl alcohol oxidation

Fig. 4 shows the XPS of Pd 3d region of Pd/Al_2O_3 and Pd/TiO_2 samples after different calcination pretreatments. For Pd/Al_2O_3–N and Pd/Al_2O_3–O before reaction, the peaks of binding energy are observed at 336.5 and 341.8 eV, corresponding to the PdO $3d_{5/2}$ and PdO $3d_{3/2}$, respectively. For Pd/Al_2O_3–H before reaction, the peaks of binding energy are observed at 335.2 and 340.5 eV corresponding to the Pd $3d_{5/2}$ and Pd $3d_{3/2}$, respectively [32]. After reaction of benzyl alcohol oxidation, the peaks of binding energy at 335.2, 337.2, 340.5 and 342.5 eV can be observed for Pd/Al_2O_3 calcined under different atmospheres. The peaks of binding energy at 335.2 and 340.5 eV are assigned to $3d_{5/2}$ and $3d_{3/2}$ of metallic Pd, while the peaks of binding energy at 337.2 and 342.5 eV are assigned to $3d_{5/2}$ and $3d_{3/2}$ of hydrated or coordinated Pd^{2+} [33,34]. Both Pd^{2+} and Pd^0 species exist in Pd/Al_2O_3 after benzyl alcohol oxidation reaction, no matter what the initial Pd species are. The changes in the valance states of palladium species in Pd/Al_2O_3 catalysts during benzyl alcohol oxidation are quite evident. Meanwhile, the XPS in O 1s region do not show obvious changes for Pd/Al_2O_3 samples before and after reaction (Fig. S2).

Compared to Pd/Al_2O_3, the circumstances on Pd/TiO_2 are a bit more complicated. For Pd/TiO_2–N and Pd/TiO_2–O, PdO_x ($1 < x < 2$) are observed as exclusive species before reaction. Based on the preparation process, palladium species should exist in the form of palladium oxide, similar to the cases of Pd/Al_2O_3–N and Pd/Al_2O_3–O. While high temperature treatments at 673 K cause the electrons transfer from palladium species to adjacent surface TiO_2 and therefore palladium oxides are oxidized to higher valence, accompanied by the partial reduction of Ti^{IV} to Ti^{III} (Fig. S3). For Pd/TiO_2–H, both PdO_x and metallic palladium are observed before reaction. After benzyl alcohol oxidation, the valance states of palladium species changes and metallic palladium together with ionic Pd^{2+} can be observed for all Pd/TiO_2 samples.

FTIR spectroscopy with CO as probe is informative and sensitive technique for the characterization of palladium sites. The characteristic of this technique lies in that only exposed palladium sites can be explored, while palladium sites in sub-surface position or buried inside cannot be explored. Thus, it can provide us with straightforward information on the available palladium sites in the catalytic reactions. Fig. 5 shows the FTIR spectra of CO saturated adsorption on Pd/Al_2O_3 and Pd/TiO_2 at room temperature. For Pd/Al_2O_3–O before reaction, a strong band at 1925 cm^{-1} and three weak bands at 2170, 2120 and 2090 cm^{-1} can be observed. The band at 1925 cm^{-1} is assigned to bridge-bonded CO on Pd (1 1 1), while the band at 2090 cm^{-1} is assigned to atop-bonded CO on the Pd (1 1 1) defects [35]. The band at 2170 cm^{-1} is assigned to linear-bonded CO on ionic Pd^{2+} and band at 2120 cm^{-1} is assigned to linear-bonded CO on ionic Pd^+ [36,37]. For Pd/Al_2O_3–N before reaction, a strong band at 1925 cm^{-1} and four weak bands at 2170, 2120, 2090 and 1990 cm^{-1} can be observed. The band at 1990 cm^{-1} is assigned to bridge-bonded CO on Pd (1 0 0) [38,39]. Based on the pretreatment processes and the XPS results, palladium species should exist in the oxide form in Pd/Al_2O_3–N and Pd/Al_2O_3–O. While these palladium species can be reduced to metallic palladium during the process of CO adsorption. For Pd/Al_2O_3–H before reaction, bridge-bonded CO on Pd (1 1 1) (band at 1930 cm^{-1}), bridge-bonded CO on Pd (1 0 0) (band at 1990 cm^{-1}) and atop-bonded CO on Pd (1 1 1) defects (band at 2090 cm^{-1}) are observed during CO adsorption. After the reaction of benzyl alcohol oxidation, the adsorption behaviours of CO on palladium species change greatly. For Pd/Al_2O_3–H after reaction, linear-bonded CO on ionic palladium oxides (band at 2170 and 2020 cm^{-1}) and atop-bonded CO on Pd (1 1 1) defects (2095 cm^{-1}) are observed. For Pd/Al_2O_3–N and Pd/Al_2O_3–O after reaction, linear-bonded CO on ionic palladium oxides (band at 2170 and 2020 cm^{-1}) and atop-bonded CO on Pd (1 1 1) defects (2095 cm^{-1}), together with bridge-bonded (1930 cm^{-1}) and threefold hollow-bonded (1890 cm^{-1}) CO on Pd (1 1 1), can be observed. The XPS results indicate that after reaction the majority of palladium species exist in the form of metallic palladium, with a small quantity in the form of ionic Pd^{2+}. The formation of ionic Pd^{2+} is supported by the results from FTIR spectra of CO adsorption. A summary of IR bands observed during CO adsorption is shown in Table 2. The results from FTIR spectroscopy with CO as probe on Pd/TiO_2 are substantially similar to those on Pd/Al_2O_3 and a concise summary is shown in Table 3.

The palladium species in supported Pd catalysts, i.e. Pd/Al_2O_3 and Pd/TiO_2, undergo obvious reconstruction during reaction of

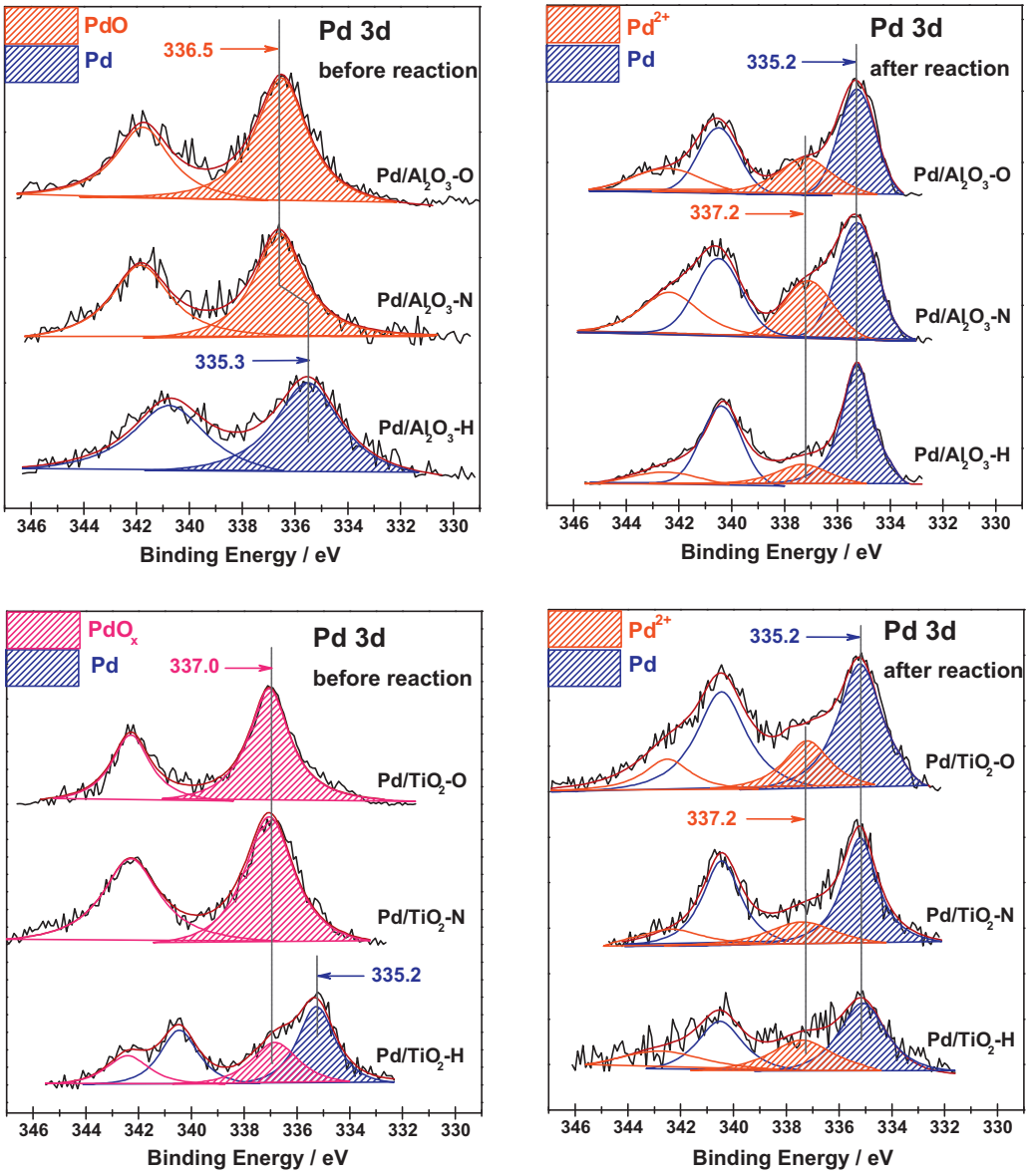

Fig. 4. XPS of Pd 3d region of Pd/Al_2O_3 and Pd/TiO_2 before and after reaction.

benzyl alcohol oxidation under our reaction conditions. On one hand, the bulk valance states of palladium change, as confirmed by XPS results. On the other hand, the surface morphologies of palladium particles change, as probed by FTIR spectra with CO adsorption. The reconstruction of palladium species is also supported by the different O_2-TPD profiles of supported Pd catalysts before and after reaction, as seen in Fig. S4.

3.4. Active palladium sites for benzyl alcohol oxidation

Based on the literature reports, the selective oxidation of alcohols may proceed via classical two-step dehydrogenation mechanism [3]. In the first step, the O—H bond of alcohol breaks upon adsorption on the surface sites and produces alkoxide. In the second step, the β-C—H bond in alkoxide is preferentially broken, facilitated by the electron-withdrawing effect of the oxygen atom. The role of oxygen is to oxidize the co-product hydrogen and thus shift the equilibrium toward the carbonyl compound [41–43].

During the reaction of benzyl alcohol oxidation over supported Pd catalysts, palladium sites undergo obvious reconstruction. For Pd/Al_2O_3–N and Pd/Al_2O_3–O, palladium oxides are reduced to metallic palladium during reaction. Under solvent-free reaction conditions, the initial reduction of palladium oxides can only be caused by the adsorbed benzyl alcohol. That is, benzyl alcohol adsorbs on the palladium oxide during reaction and subsequently reduces of most palladium oxides to metallic palladium (a small amount of palladium species remains in the form of palladium oxides), accompanied by the oxidation of benzyl alcohol to benzyl alkoxide. It should be mentioned that palladium oxides located at outer surface of clusters could be reduced by benzyl alcohol, while those buried inside cannot be reduced due to the steric effect. However, the majority of palladium oxides are indeed reduced to metallic palladium after reaction (Fig. 4). The most reasonable explanation is that β-C—H bond in benzyl alkoxide breaks on palladium sites and the as-produced active hydrogen subsequently reduces most palladium oxides buried inside clusters to metallic palladium through spill over. Meanwhile, the benzaldehyde is released to the liquid phase as the final product. After the reconstruction of Pd sites is accomplished, the oxidation of benzyl alcohol will proceed via the classical two-step dehydrogenation pathway.

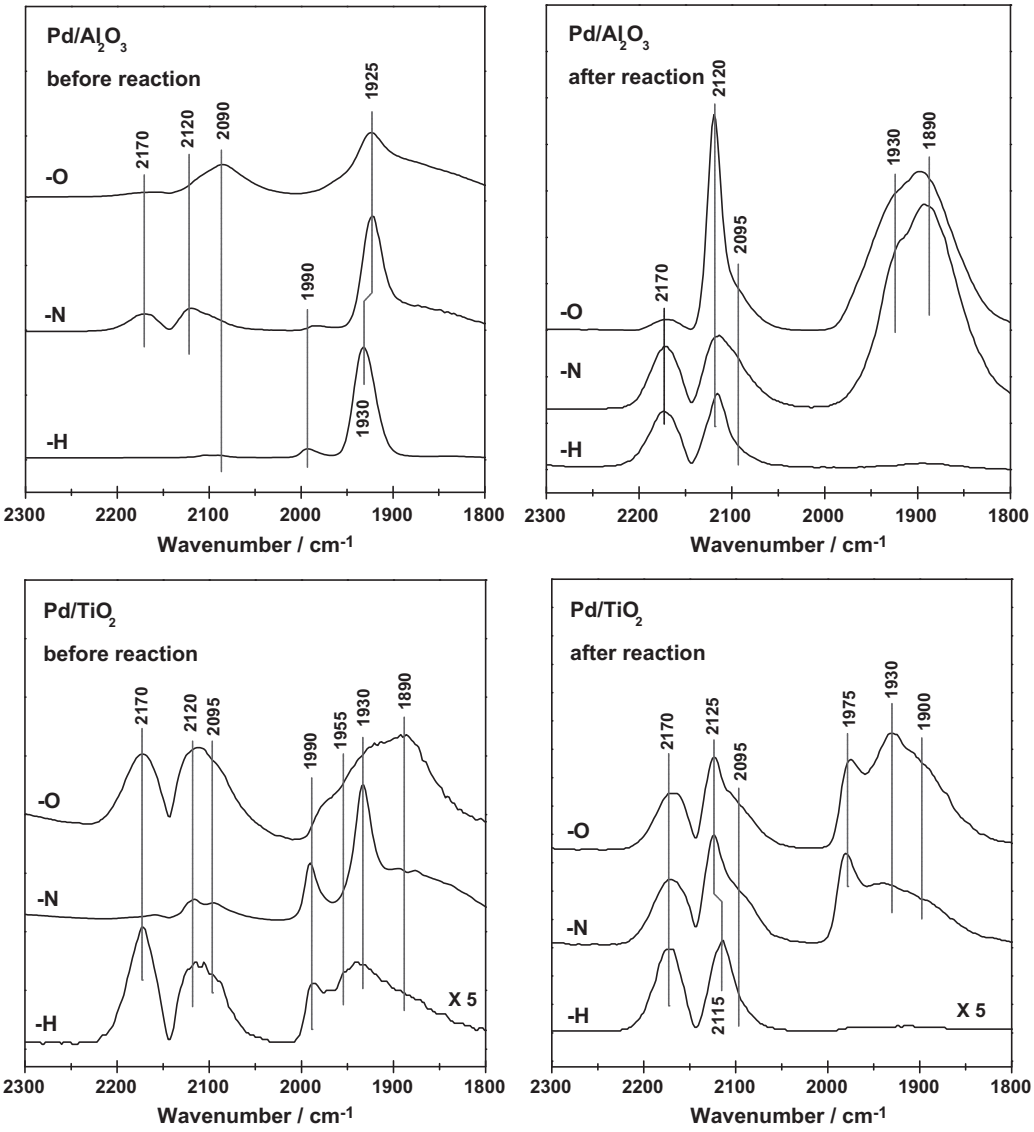

Fig. 5. FTIR spectra of CO adsorption on Pd/Al_2O_3 and Pd/TiO_2 before and after reaction.

For Pd/Al_2O_3–H, palladium species exist in the metallic form and the oxidation of benzyl alcohol can proceed directly via the classical two-step dehydrogenation pathway. The initiating step for benzyl alcohol selective oxidation over supported Pd catalysts with palladium oxide as initial species is described in Fig. 6.

Based on the proposed reaction pathways, it appears that the reduction of palladium oxide to metallic palladium by adsorbed benzyl alcohol is an essential step for benzyl alcohol oxidation over Pd/Al_2O_3–N and Pd/Al_2O_3–O. The oxidation of benzyl alcohol over Pd/Al_2O_3–N and Pd/Al_2O_3–H at different temperatures are performed and the results are summarized in Table 4. It is seen that very low TOF values are obtained on Pd/Al_2O_3–N with palladium oxide as initial species at below 373 K, when palladium oxides cannot be reduced by benzyl alcohol. In contrast, much higher TOF values can be achieved on Pd/Al_2O_3–H with metallic palladium as initial species at the same reaction temperature. These results strongly support that metallic palladium species are much more active than palladium oxides, in consistent with the results reported by Grunwaldt et al. [29]. The in situ reduction of palladium oxides to metallic palladium is the main cause leading to the controversies. It is worthy of noting that when Pd/Al_2O_3–N after reconstruction, e.g. after reaction at 393 K for 8 h, is employed as catalyst for benzyl alcohol oxidation at 363 K, high TOF value of 1209 mol/h mol_{Pd} can be obtained.

Vide supra, metallic palladium species are more active than palladium oxides for benzyl alcohol oxidation over Pd catalysts under our reaction conditions. Therefore, a key question arises on the primary palladium site for alcohol oxidation. Since palladium sites undergo reconstruction during reaction, it is more instructive to focus on the surface palladium sites in supported Pd catalysts after reaction than those before reaction. For Pd/Al_2O_3 after reaction, three main types of exposed metallic palladium sites are observed: the defect sites, the bridge sites and the hollow sites on Pd (1 1 1). It have been reported that the oxidative dehydrogenation of alcohol to corresponding aldehyde occurred on all exposed metallic palladium faces, whereas the undesired product decarbonylation occurred preferentially on hollow sites on Pd (1 1 1) faces [44]. While in our experiments, almost no decarbonylation product can be detected during reaction. It is well known that the bond breaking is facilitated by defects [45,46]. Therefore, we propose that the defect sites on Pd (1 1 1) are the primary sites for benzyl alcohol oxidation. By calculation the

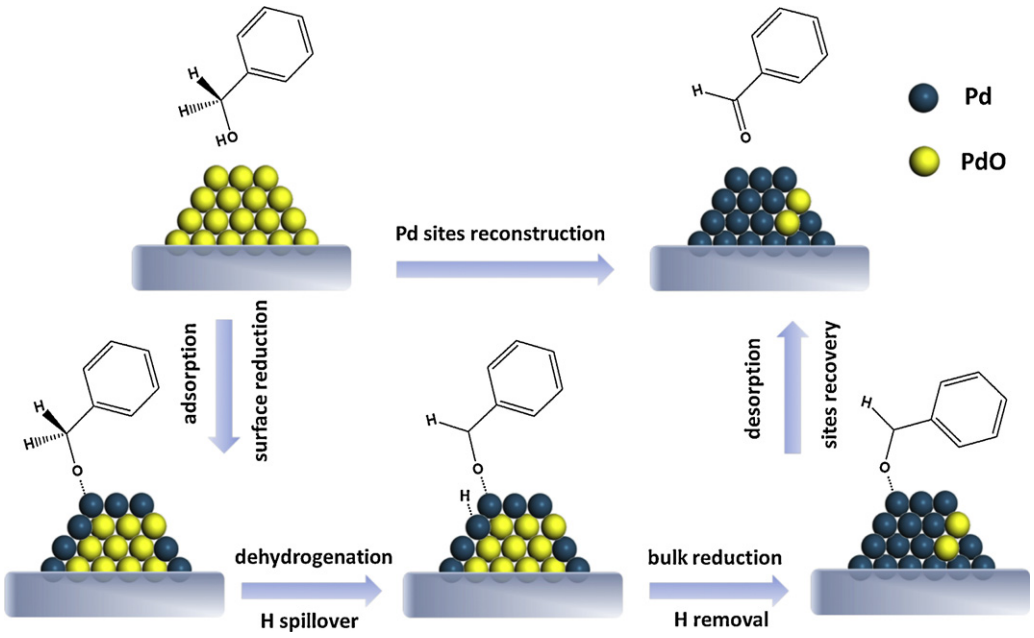

Fig. 6. Initiating step for benzyl alcohol selective oxidation over supported Pd catalysts with palladium oxides as initial palladium species.

Table 2
Summary of bands observed during CO saturated adsorption on Pd/Al_2O_3 at room temperature.

Sample	Wavenumber (cm^{-1})	Assignment
Pd/Al_2O_3–O before reaction	2170	Linear-bonded CO on ionic Pd^{2+}
	2120	Linear-bonded CO on ionic Pd^{+}
	2090	A top-bonded CO on Pd (1 1 1) defects
	1925	Twofold bridge-bonded CO on Pd (1 1 1)
Pd/Al_2O_3–O after reaction	2170	Linear-bonded CO on ionic Pd^{2+}
	2120	Linear-bonded CO on ionic Pd^{+}
	2095	A top-bonded CO on Pd (1 1 1) defects
	1930	Bridge-bonded CO on Pd (1 1 1)
	1890	Threefold hollow-bonded CO on Pd (1 1 1)
Pd/Al_2O_3–N before reaction	2170	Linear-bonded CO on ionic Pd^{2+}
	2120	Linear-bonded CO on ionic Pd^{+}
	2090	A top-bonded CO on Pd (1 1 1) defects
	1990	Bridge-bonded CO on Pd (1 0 0)
	1925	Bridge-bonded CO on Pd (1 1 1)
Pd/Al_2O_3–N after reaction	2170	Linear-bonded CO on ionic Pd^{2+}
	2120	Linear-bonded CO on ionic Pd^{+}
	2095	A top-bonded CO on Pd (1 1 1) defects
	1930	Bridge-bonded CO on Pd (1 1 1)
	1890	Threefold hollow-bonded CO on Pd (1 1 1)
Pd/Al_2O_3–H before reaction	2090	A top-bonded CO on Pd (1 1 1) defects
	1990	Bridge-bonded CO on Pd (1 0 0)
	1930	Bridge-bonded CO on Pd (1 1 1)
Pd/Al_2O_3–H after reaction	2170	Linear-bonded CO on ionic Pd^{2+}
	2120	Linear-bonded CO on ionic Pd^{+}
	2095	A top-bonded CO on Pd (1 1 1) defects

Table 3
Summary of bands observed during CO saturated adsorption on Pd/TiO_2 at room temperature.

Sample	Wavenumber (cm^{-1})	Assignment
Pd/TiO_2–O before reaction	2170	Linear-bonded CO on ionic Pd^{2+}
	2120	Linear-bonded CO on ionic Pd^{+}
	2095	A top-bonded CO on Pd (1 1 1) defects
	1990	Bridge-bonded CO on Pd (1 0 0)
	1955	Bridge-bonded CO on Pd particle edges [40]
	1930	Bridge-bonded CO on Pd (1 1 1)
	1890	Threefold hollow-bonded CO on Pd (1 1 1)
Pd/TiO_2–O after reaction	2170	Linear-bonded CO on ionic Pd^{2+}
	2125	Linear-bonded CO on ionic Pd^{+}
	2095	A top-bonded CO on Pd (1 1 1) defects
	1975	Bridge-bonded CO on Pd particle edges
	1930	Bridge-bonded CO on Pd (1 1 1)
	1900	Threefold hollow-bonded CO on Pd (1 1 1)
Pd/TiO_2–N before reaction	2120	Linear-bonded CO on ionic Pd^{+}
	2095	A top-bonded CO on Pd (1 1 1) defects
	1990	Bridge-bonded CO on Pd (1 0 0)
	1930	Bridge-bonded CO on Pd (1 1 1)
	1890	Threefold hollow-bonded CO on Pd (1 1 1)
Pd/TiO_2–N after reaction	2170	Linear-bonded CO on ionic Pd^{2+}
	2125	Linear-bonded CO on ionic Pd^{+}
	2095	A top-bonded CO on Pd (1 1 1) defects
	1975	Bridge-bonded CO on Pd particle edges
	1930	Bridge-bonded CO on Pd (1 1 1)
	1900	Threefold hollow-bonded CO on Pd (1 1 1)
Pd/TiO_2–H before reaction	2170	Linear-bonded CO on ionic Pd^{2+}
	2120	Linear-bonded CO on ionic Pd^{+}
	2095	A top-bonded CO on Pd (1 1 1) defects
	1990	Bridge-bonded CO on Pd (1 0 0)
	1955	Bridge-bonded CO on Pd particle edges
	1930	Bridge-bonded CO on Pd (1 1 1)
	1890	Threefold hollow-bonded CO on Pd (1 1 1)
Pd/TiO_2–H after reaction	2170	Linear-bonded CO on ionic Pd^{2+}
	2115	Linear-bonded CO on ionic Pd^{+}
	2095	A top-bonded CO on Pd (1 1 1) defects

Table 4
Selective oxidation of benzyl alcohol over Pd/Al_2O_3–N and Pd/Al_2O_3–H.

Catalyst	Reaction temperature (K)	Conversion (%)[a]	Product selectivity (%)		TOF[c] (mol/h mol_{Pd})
			Benzaldehyde	Carbonyls[b]	
Pd/Al_2O_3–N	353	1.4	95.2	99.9	63
	363	2.1	94.1	99.9	95
	373	19.5	93.6	99.9	880
	383	64.4	91.7	99.9	2906
	393	80.1	94.3	99.9	3615
	363[d]	26.8	95.2	99.9	1209
Pd/Al_2O_3–H	353	4.7	94.1	99.9	212
	363	29.8	95.3	99.9	1345
	373	63.5	96.5	99.9	2865
	383	57.8	92.8	99.9	2608
	393	35.2	95.2	99.9	1588

[a]Conversion after time-on-stream of 8 h.
[b]Including benzaldehyde, benzoic acid and benzylbenzoate.
[c]Calculated as the ratio of moles of benzyl alcohol converted per mole of total Pd per hour, measured at time-on-stream of 30 min.
[d]Reuse of Pd/Al_2O_3–N after reaction at 393 K for 8 h.

relative intensities of corresponding FTIR bands in K-M function, the percentage of defect sites in all exposed Pd (1 1 1) is determined to be Pd/Al_2O_3–N > Pd/Al_2O_3–O > Pd/Al_2O_3–H after reaction (Fig. 5), in good agreement with their activity order (Fig. 3). While for Pd/TiO_2, similar activity is obtained on Pd/TiO_2–N and Pd/TiO_2–O with similar percentage of defect sites in exposed Pd (1 1 1). The good correlation between activity and exposed defect sites strongly proves that the defect sites on Pd (1 1 1) are the primary sites for benzyl alcohol oxidation. In the present study, pretreating supported Pd catalysts in oxidizing or inert atmosphere and subsequent reducing of Pd species in situ by reactant alcohol can create a higher amount of defect sites than pretreating Pd catalysts in reducing atmosphere. Therefore, the activity of supported Pd catalysts in the selective oxidation of alcohols can be enhanced via the in situ reduction pathway.

4. Conclusions

The present work shows that the selective oxidation of benzyl alcohol to benzaldehyde can be realized on Pd/Al_2O_3 and Pd/TiO_2 catalysts with high activity and selectivity via ideal green oxidation process, i.e. under solvent-free conditions and with molecular oxygen as oxidant. The calcination pretreatments of supported Pd catalysts show great effects on catalytic activity. The palladium sites in supported Pd catalysts undergo reconstruction during benzyl alcohol oxidation under reaction conditions employed in this study, as indicated by the analysis results from XPS, FTIR spectra of CO adsorption and O_2-TPD. Metallic palladium species are proved to be more active than palladium oxides for benzyl alcohol oxidation over Pd catalysts. While the reduction of palladium oxides to metallic palladium by adsorbed benzyl alcohol, i.e. the reconstruction of palladium sites, is an essential step for benzyl alcohol oxidation over supported Pd catalyst with palladium oxides as initial palladium species. The defect sites on Pd (1 1 1) are proposed to be the primary sites for benzyl alcohol oxidation based on the correlation between catalytic activity and the percentage of exposed defect sites in palladium clusters. The in situ reduction of palladium species by reactant alcohols is found to be an efficient pathway to create more defect sites, which leads to higher activity of supported Pd catalysts in the selective oxidation of benzyl alcohol.

Acknowledgments

This work is supported by the National Basic Research Program of China (2009CB623502), NCET of Ministry of Education (NCET-11) and MOE (IRT0927). The support from the State Key Laboratory of Catalytic Materials and Reaction Engineering (RIPP, SINOPEC) is also acknowledged.

Appendix A. Supplementary data

Supplementary data associated with this article can be found, in the online version, at doi:10.1016/j.apcatb.2011.12.011.

References

[1] R.A. Sheldon, I.W.C.E. Arends, A. Dijksman, Catal. Today 57 (2000) 157–166.
[2] R.A. Sheldon, I.W.C.E. Arends, G.J. ten Brink, A. Dijksman, Acc. Chem. Res. 35 (2002) 774–781.
[3] T. Mallat, A. Baiker, Chem. Rev. 104 (2004) 3037–3058.
[4] B.Z. Zhan, A. Thompson, Tetrahedron 60 (2004) 2917–2935.
[5] M.J. Schultz, M.S. Sigman, Tetrahedron 62 (2006) 8227–8241.
[6] Y.C. Son, V.D. Makwana, A.R. Howell.S.L., Angew. Chem. Int. Ed. 40 (2001) 4280–4283.
[7] J. Zhu, K. Kailasam, A. Fischer, A. Thomas, ACS Catal. 1 (2011) 342–347.
[8] K. Yamaguchi, K. Mori, T. Mizugaki, K. Ebitani, K. Kaneda, J. Am. Chem. Soc. 122 (2000) 7144–7145.
[9] K. Yamaguchi, N. Mizuno, Chem. Eur. J. 9 (2003) 4353–4361.
[10] A. Kockritz, M. Sebek, A. Dittmar, J. Radnik, A. Bruckner, U. Bentrup, M.M. Pohl, H. Hugl, W. Magerlein, J. Mol. Catal. A 246 (2006) 85–99.
[11] K. Yamaguchi, J.W. Kim, J. He, N. Mizuno, J. Catal. 268 (2009) 343–349.
[12] V.R. Choudhary, A. Dhar, P. Jana, R. Jha, B.S. Uphade, Green Chem. 7 (2005) 768–770.
[13] A. Abad, P. Concepcion, A. Corma, H. Garcia, Angew. Chem. Int. Ed. 44 (2005) 4066–4069.
[14] C.D. Pina, E. Falletta, L. Prati, M. Rossi, Chem. Soc. Rev. 37 (2008) 2077–2095.
[15] L.C. Wang, Y.M. Liu, M. Chen, Y. Cao, H.Y. He, K.N. Fan, J. Phys. Chem. C 112 (2008) 6981–6987.
[16] F.Z. Su, Y.M. Liu, L.C. Wang, Y. Cao, H.Y. He, K.N. Fan, Angew. Chem. Int. Ed. 47 (2008) 334–337.
[17] C.Y. Ma, B.J. Dou, J.J. Li, J. Cheng, Q. Hu, Z.P. Hao, S.Z. Qiao, Appl. Catal. B 92 (2009) 202–208.
[18] K.M. Choi, T. Akita, T. Mizugaki, K. Ebitani, K. Kaneda, New J. Chem. 27 (2003) 324–328.
[19] K. Mori, T. Hara, T. Mizugaki, K. Ebitani, K. Kaneda, J. Am. Chem. Soc. 126 (2004) 10657–10666.
[20] T.L. Stuchinskaya, I.V. Kozhevnikov, Catal. Commun. 4 (2003) 417–422.
[21] U.R. Pillai, E. Sahle-Demessie, Green Chem. 6 (2004) 161–165.
[22] M.S. Kwon, N. Kim, C.M. Park, J.S. Lee, K.Y. Kang, J. Park, Org. Lett. 7 (2005) 1077–1079.
[23] J. Chen, Q.H. Zhang, Y. Wang, H.L. Wan, Adv. Synth. Catal. 350 (2008) 453–464.
[24] H. Wang, S.X. Deng, Z.R. Shen, J.G. Wang, D.T. Ding, T.H. Chen, Green Chem. 11 (2009) 1499–1502.
[25] T. Harada, S. Ikeda, F. Hashimoto, T. Sakata, K. Ikeue, T. Torimoto, M. Matsumura, Langmuir 26 (2010) 17720–17725.
[26] C. Keresszegi, J.D. Grunwaldt, T. Mallat, A. Baiker, J. Catal. 222 (2004) 268–280.
[27] A.F. Lee, K. Wilson, Green Chem. 6 (2004) 37–42.
[28] A.F. Lee, S.F.J. Hackett, J.S.J. Hargreaves, K. Wilson, Green Chem. 8 (2006) 549–555.
[29] J.D. Grunwaldt, M. Caravati, A. Baiker, J. Phys. Chem. B 110 (2006) 25586–25589.
[30] S.J. Tauster, Acc. Chem. Res. 20 (1987) 389–394.
[31] Q. Fu, T. Wagner, S. Olliges, H.-D. Carstanjen, J. Phys. Chem. B 109 (2005) 944–951.

[32] C.D. Wagner, W.M. Riggs, L.E. Davis, J.F. Moulder, G.E. Muilenberg, Handbook of X-ray Photoelectron Spectroscopy: A Reference Book of Standard Data for Use in X-ray Photoelectron Spectroscopy, Perkin-Elmer MN, Eden-Prairie, 1979.
[33] N.S. Babu, N. Lingaiah, R. Gopinath, P.S.S. Reddy, P.S.S. Prasad, J. Phys. Chem. C 111 (2007) 6447–6453.
[34] L. Chen, A. Yelon, E. Sacher, J. Phys. Chem. C 115 (2011) 7896–7905.
[35] D.R. Rainer, M.-C. Wu, D.I. Mahon, D.W. Goodman, J. Vaccine Sci. Technol. A 14 (1996) 1184–1188.
[36] W. Juszczyk, Z. Karpinski, I. Ratajczykowa, Z. Stanasiuk, J. Zielinki, L.L. Sheu, W.M.H. Sachtler, J. Catal. 120 (1989) 68–77.
[37] D. Tessier, A. Rakai, F. Bozon-Verduraz, J. Chem. Soc., Faraday Trans. 88 (1992) 741–749.
[38] T. Lear, R. Marshall, J.A. Lopez-Sanchez, S.D. Jackson, T.M. Klapötke, M. Bäumer, G. Rupprechter, H.J. Freund, D. Lennon, J. Chem. Phys. 123 (2005) 174706–174713.
[39] M. Frank, M. Bäumer, Phys. Chem. Chem. Phys. 2 (2000) 3723–3737.
[40] F. Di Gregorio, L. Bisson, T. Armaroli, C. Verdon, L. Lemaitre, C. Thomazeau, Appl. Catal. A 352 (2009) 50–60.
[41] R. DiCosimo, G.M. Whitesides, J. Phys. Chem. 93 (1989) 768–775.
[42] P. Vinke, H.E. van Dam, H. van Bekkum, Stud. Surf. Sci. Catal. 55 (1990) 147–158.
[43] H.E. van Dam, L.J. Wisse, H. van Bekkum, Appl. Catal. 61 (1990) 187–197.
[44] D. Ferri, C. Mondelli, F. Krumeich, A. Baiker, J. Phys. Chem. B 110 (2006) 22982–22986.
[45] G. Ertl, Adv. Catal. 45 (2000) 1–69.
[46] B. Hammer, J.K. Norskov, Adv. Catal. 45 (2000) 71–129.